Journal of
Nanophotonics

Nanophotonics.SPIEDigitalLibrary.org

Loss analysis in nitride deep ultraviolet planar cavity

Zhongming Zheng
Yingqian Li
Onkundi Paul
Hao Long
Samuel Matta
Mathieu Leroux
Julien Brault
Leiying Ying
Zhiwei Zheng
Baoping Zhang

SPIE.

Zhongming Zheng, Yingqian Li, Onkundi Paul, Hao Long, Samuel Matta, Mathieu Leroux, Julien Brault, Leiying Ying, Zhiwei Zheng, Baoping Zhang, "Loss analysis in nitride deep ultraviolet planar cavity," *J. Nanophoton.* **12**(4), 043504 (2018), doi: 10.1117/1.JNP.12.043504.

Loss analysis in nitride deep ultraviolet planar cavity

Zhongming Zheng,[a] Yingqian Li,[a] Onkundi Paul,[a] Hao Long,[a,*] Samuel Matta,[b] Mathieu Leroux,[b] Julien Brault,[b] Leiying Ying,[a] Zhiwei Zheng,[a] and Baoping Zhang[a,*]

[a]Xiamen University, Optoelectronics Engineering Research Center, Department of Electronic Engineering, Xiamen, China

[b]Université Côte d'Azur, CNRS, CRHEA, Valbonne, France

Abstract. In recent decades, literatures about visible vertical cavity surface emitting lasers (VCSELs) have been reported. However, due to high optical loss in the cavity, lasing from deep ultraviolet (DUV) VCSEL was still rarely achieved. The optical loss in nitride DUV microcavity was analyzed in detail. DUV nitride vertical Fabry–Pérot microcavity with active layer of AlGaN-based quantum dots and double-side HfO_2/SiO_2 distributed bragger reflectors was fabricated. Optical losses with of the order of $10^3\ cm^{-1}$ were deduced from the Q value of the cavity modes. The main origination of optical loss in DUV cavity was calculated and ascribed to the interface scattering. The interface roughness appearing after laser lift-off process and overlap between rough interface and standing optical wave were two key parameters that contributed to interface scattering loss. We believe that our results will provide useful information for improving DUV VCSEL devices. © *2018 Society of Photo-Optical Instrumentation Engineers (SPIE)* [DOI: 10.1117/1.JNP.12.043504]

Keywords: deep ultraviolet; microcavity; interface scattering; AlGaN quantum dots.

Paper 18065SS received Apr. 13, 2018; accepted for publication May 3, 2018; published online May 18, 2018.

1 Introduction

$Al_xGa_{1-x}N$ alloys, with its direct bandgap ranging from 3.4 to 6.0 eV by adjusting Al concentration,[1] have attracted a lot of attention for its promising application in high density optical storage, water sterilization, biological detection, and photolithography. In the last few decades, AlGaN-based deep ultraviolet (DUV) edge-emitting lasers from 214 to 368.4 nm have been demonstrated.[2–14]

Comparing with edge-emitting lasers, DUV vertical cavity surface emitting lasers (VCSELs) own many advantages, such as low power consumption, large-scale two-dimensional (2-D) array feasibility, single longitudinal mode, and circular far-field beam.[15] The development of DUV VCSELs will benefit extensive applications in high resolution photolithography, biological disinfection, medical therapy, data communication, etc. VCSELs were proposed by Iga et al.,[16–18] and initially obtained near 1.2 μm in 1979 at 77 K.[19] In recent years, VCSELs have been successfully progressed to blue and green spectrums using III-nitride semiconductors.[20–26] However, there were rare literatures about VCSELs operating in the UV regime,[27–30] and none has reported in the DUV (<320 nm) range. Distributed Bragg reflector (DBR) structure is one of the most essential modules in DUV VCSELs fabrication. One typical VCSEL structure was based on the active epilayer grown on bottom nitride DBR and followed by top dielectric or nitride DBR.[28,30] However, the nitride DBR generally suffered by small refractive index contrast and narrow reflectivity bandwidth. To get necessary reflectivity (>99%), extremely high period number of nitride DBR (>40 pairs) was needed. This increases the difficulty in material growth and fabrication of DUV VCSELs. By contrast, double-side dielectric DBR structures, with larger

*Address all correspondence to: Hao Long, E-mail: longhao@xmu.edu.cn; Baoping Zhang, E-mail: bzhang@xmu.edu.cn

1934-2608/2018/$25.00 © 2018 SPIE

refractive index contrast between two oxide layers, are therefore more preferable. However, double-side dielectric DBR structures introduced complex and delicate laser lift-off (LLO) process, making devices suffered severe optical loss. Optical loss was a key problem in DUV VCSELs. Large optical loss brings unaffordable high lasing threshold or even no lasing action.

In this work, we analyzed the optical loss in nitride DUV vertical microcavity based on double-side dielectric DBRs. The intrinsic originations of optical loss were identified. Four discrete cavity modes from 305 nm to 335 nm were observed. Optical losses of DUV cavity modes were analyzed to be in the 10^3 cm^{-1} range. Theoretical calculation shows that the scattering loss from the interface by laser lift-off is the main cause for cavity loss, which was strongly related to the interface roughness and the overlap between rough interface and stationary optical field.

2 Experiment Details

The AlGaN quantum dots (QDs) epilayer was grown on c-plane sapphire substrate by molecular beam epitaxy (MBE) in a RIBER 32 P reactor, following the growth conditions described in Ref. 31. As shown in Fig. 1(a), the 30 nm GaN layer and 120 nm AlN layer were used as buffer layers. The active layer consists of ten monolayers of $Al_{0.2}Ga_{0.8}N$ quantum dots sandwiched by $Al_{0.7}Ga_{0.3}N$ barrier layers. Fabrication of the vertical microcavity was then carried out with the first step of coating 15 pairs of HfO_2/SiO_2 bottom-DBR on the top of epilayer. The peak reflectivity (98.01%) and bandwidth (~70 nm) of our oxide DBR were superior to the ones of nitride DBR.[30] After that, the bottom DBR side of sample was wax bonded to a quartz glass. LLO was sequentially performed with a 248-nm KrF excimer laser to remove the sapphire substrate. During the LLO process, the 30-nm GaN buffer layer was decomposed into melted Ga and nitrogen gas. The molten Ga was then dissolved by diluted hydrochloric acid. After that, a 10.5 pairs of HfO_2/SiO_2 top-DBR, with a peak reflectivity of 96.81% and bandwidth of 69 nm, were deposited on the exposed AlN layer. Photoluminescence (PL) measurements were performed using the 266-nm Nd:YAG laser as pumping source. The schematic diagram of the PL set-up is depicted in Fig. 1(c).

3 Results and Discussion

The PL results are depicted in Fig. 2. Four cavity modes are clearly observed at 305, 314, 323, and 335 nm. Interval among these modes is around 10 nm. The quality factor (Q value) of every mode can be calculated according to Eq. (1):

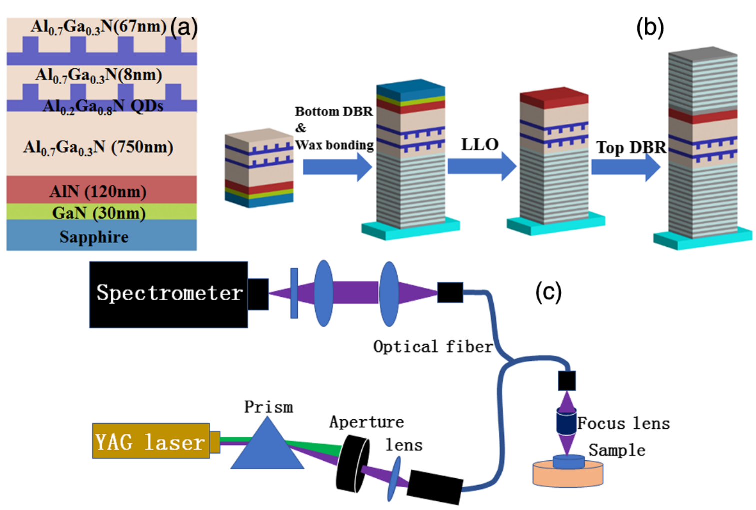

Fig. 1 (a) Structure of the DUV epilayer; (b) fabrication processes of DUV vertical cavity; and (c) PL set-up used in this study.

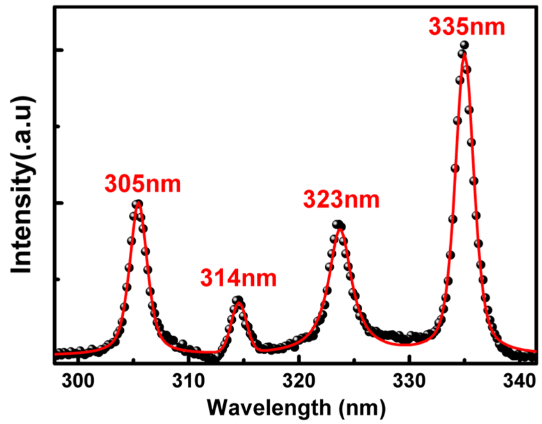

Fig. 2 Emission spectra of the microcavity at room temperature.

$$Q = \lambda_0/\Delta\lambda, \tag{1}$$

where λ_0 is the peak wavelength of the emission mode and $\Delta\lambda$ is full width of half maximum of peak.

The Q values of DUV cavity modes were small compared with visible ones,[32] indicating strong optical losses in the cavity. These optical losses can be deduced from Q according to Eq. (2):

$$Q = 2\pi \frac{nL_{\mathrm{eff}}}{\lambda}\left[\frac{1}{\ln(R_{b\_\mathrm{DBR}}R_{t\_\mathrm{DBR}})^{-1/2} + L_{\mathrm{eff}}\alpha}\right], \tag{2}$$

where n is the cavity refractive index, L_{eff} is the effective cavity length, λ is the wavelength, α is the internal cavity loss, and R_{t_DBR} and R_{b_DBR} are the top and bottom DBR reflectivity, respectively. The effective cavity length L_{eff} can be obtained from Eq. (3):

$$v_{q+1} - v_q = \frac{c}{2nL_{\mathrm{eff}}}, \tag{3}$$

where q is the longitudinal mode order, ν is the longitudinal mode frequency, and c is the vacuum light velocity. L_{eff} was evaluated to be 2288 nm. Therefore, the cavity losses of every mode were 2671.8, 3421.9, 2102.5, and 2363.5 cm^{-1} for the 305, 314, 323, and 335 nm modes, respectively (Table 1). The cavity loss strongly affects the quality of cavity. If the cavity loss was reduced to 195 cm^{-1}, the Q value will reach 1500.

Figure 3 depicts the simulated stationary optical field distributions of each mode along with the refractive index profile. The confinement factors (Γ_r) are obtained by Eq. (4):

$$\Gamma_r = \frac{L_{\mathrm{eff}}}{d_a}\frac{\int_{d_a}|E(z)|^2\mathrm{d}z}{\int_{L_{\mathrm{eff}}}|E(z)|^2\mathrm{d}z}, \tag{4}$$

where d_a is active region thickness, $E(z)$ is the electric field intensity along the z axis, and Γ_r represents the coupling strength between active gain medium with standing wave. A Γ_r value

Table 1 *Q* values, cavity losses, and confinement factors of every cavity mode.

Mode (nm)	305	314	323	335
Q value	166.58	127.32	194.79	160.78
α (cm^{-1})	2671.8	3421.9	2102.5	2363.5
Γ_r	1.71	1.89	1.88	1.62

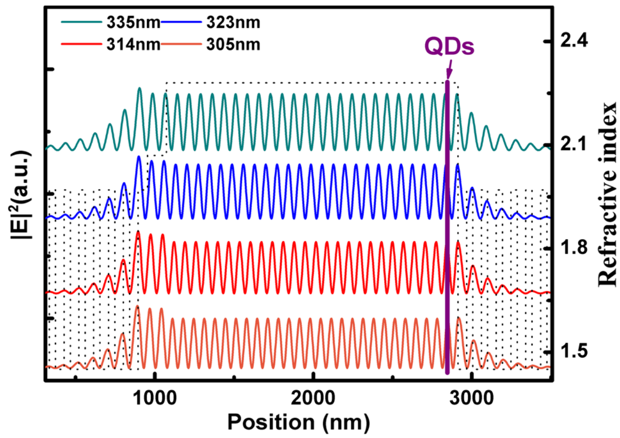

Fig. 3 Simulated stationary optical field distribution and refractive index profile in DUV cavity.

close to 2 suggests that the active region is perfectly aligned to the antinode of the cavity mode, making the most efficient coupling between gain medium and optical field. In our sample, the QD layer was artificially placed at the antinode of stationary optical field, showing confinement factor close to 2 (Table 1).

Meanwhile, the optical loss was also a significant parameter in DUV microcavity. Several factors including epilayer absorption, interface scattering, and DBR reflectivity contribute to the total optical loss. First, the $Al_{0.7}Ga_{0.3}N$ epilayer absorption was calculated based on absorption coefficient of $0.45 \times 10^3\ \mathrm{cm}^{-1}$ at 320 nm:[33]

$$A_{\mathrm{epi}} = 1 - e^{-\alpha_{\mathrm{epi}} d}, \tag{5}$$

where α_{epi} is the absorption coefficient and d is the layer thickness. The absorbance by the thickness of the epilayer was calculated and found to be 8.4%.

Second, the interface scattering was also a pivotal character in total optical loss. The interface morphology of the AlN epilayer after LLO was characterized by atomic force microscopy, as shown in Fig. 4(a). Over a 10 μm × 10 μm area, the interface was pretty rough with root mean

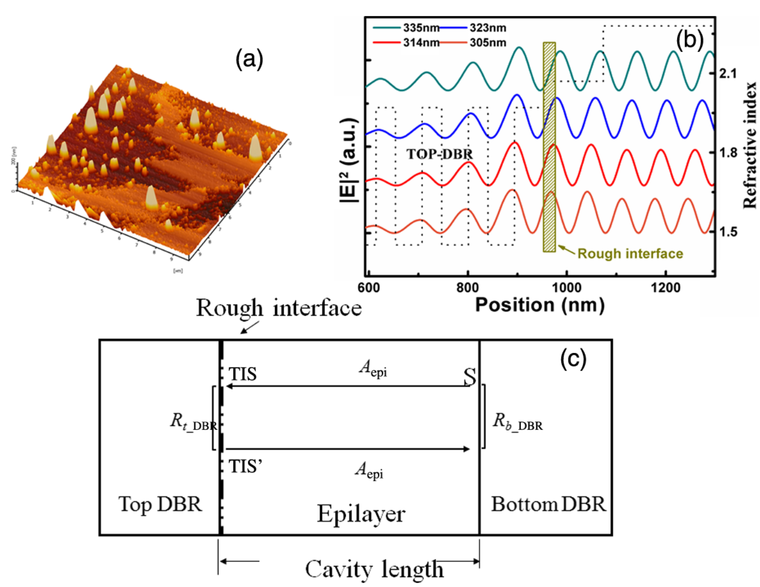

Fig. 4 (a) Atomic force microscopy image of AlN interface after LLO; (b) enlarged schematic overlap between rough interface and stationary optical field; and (c) schematic image of energy loss per single round trip.

square (RMS) roughness of 20.36 nm. The integrated scattering coefficient (ISC), i.e., the ratio between scattered and incident light intensity can be described as in Eq. (6):[34]

$$\mathrm{ISC} = C\left\{1 - \exp\left[-\left(\frac{4\pi\delta \cos\theta}{\lambda}\right)^2\right]\right\}, \tag{6}$$

where δ is the RMS of the interface, θ is the incident angle, λ is wavelength, and C is a correction factor. When light travels from epilayer to DBR, C is 0.96. If light travels from the opposite direction, C will be $1/0.96 = 1.04$. For normal incidence ($\theta = 0$), the ISC from epilayer to DBR for the 305, 314, 323, and 335-nm modes is 49%, 47%, 45%, and 42%, respectively, whereas ISC′ from DBR to epilayer is 53%, 51%, 49%, and 46%, respectively. Compared with epilayer absorption of 8.4%, the interface scattering loss (42% to 53%) dominated the cavity losses.

Meanwhile, it is worth noting that the interface scattering was also related to the overlap coefficient (β) between rough interface and stationary optical field. As shown in Fig. 4(b), the overlap coefficient was the coupling strength of the optical field with the interface roughness and could be expressed by

$$\beta = \frac{\int_0^{d_r} |E(x)|^2/|E_{\max}|^2 \, \mathrm{d}x}{d_r}, \tag{7}$$

where d_r is the thickness of rough interface and was assumed to be the RMS value of 20.36 nm; $|E(x)|^2$ and $|E_{\max}|^2$ are the electric fields along the thickness direction and maximum electric amplitude in the cavity, respectively.

The total optical loss A_{total} of all cavity modes in single round trip can be deduced by considering the average β, ISC, and ISC′ when light travels from the starting point S [Fig. 4(c)]. A_{total} is given by Eq. (8):

$$A_{\text{total}} = 1 - (1 - A_{\text{epi}})(1 - \beta * \mathrm{ISC})R_{t\_\mathrm{DBR}}(1 - \beta * \mathrm{ISC}')(1 - A_{\text{epi}})R_{b\_\mathrm{DBR}}, \tag{8}$$

where R_{b_DBR} and R_{t_DBR} are bottom and top DBR reflectivity, respectively (Table 2). It is worth mentioning that only one rough interface between top DBR and LLO interface existed. The total optical loss per round trip was thus calculated to be 67%, indicating that two thirds of light energy was consumed during one round trip. This will seriously increase the lasing threshold or even induce no lasing action if the gain medium cannot afford high injection level. Obviously, interface scattering dominated in the optical loss of the cavity. Different total losses were theoretically predicted by varying the overlap coefficient and interface roughness value. As shown in Table 3, the total optical loss can be reduced by decreasing either the overlap coefficient or the interface roughness. For instance, lowing the interface roughness to 1 nm ($0.05 \times \mathrm{RMS}$) or reducing the overlap coefficient to 5% of experimental value will reduce the optical loss from 67% to 22-25%. The Q value will also increase to about 700 correspondingly.

Therefore, to elevate the quality factor of vertical DUV microcavity, two notable actions can be implemented. First, the rough interface could be artificially placed on the wave node of standing wave to reduce overlap coefficient β. Second, the interface RMS could be refined by optimizing LLO process.

Table 2 Reflectivity of bottom and top DBRs and overlap between rough interface and standing wave.

Mode (nm)	305	314	323	335
R_{b_DBR} (%)	98.01	97.97	97.66	96.74
R_{t_DBR} (%)	96.81	96.64	95.70	91.56
β	0.94	0.84	0.68	0.32

Table 3 Total optical losses per round trip with various overlap coefficient and interface roughness. [Here, β and RMS are equal to the average value in Table 1 and Fig. 4(a)].

Interface parameters	Total loss	Interface parameters	Total loss	Interface parameters	Total loss
$\beta \times$ RMS	67%	$0.5\beta \times$ RMS	46%	$0.05\beta \times$ RMS	25%
$\beta \times$ 0.5RMS	37%	$0.5\beta \times$ 0.5RMS	30%	$0.05\beta \times$ 0.5RMS	23%
$\beta \times$ 0.25RMS	26%	$0.5\beta \times$ 0.25RMS	24%	$0.05\beta \times$ 0.25RMS	22.8%
$\beta \times$ 0.05RMS	22.2%	$0.5\beta \times$ 0.05RMS	22.1%	$0.05\beta \times$ 0.05RMS	22%

4 Conclusions

In summary, an AlGaN QDs-based vertical microcavity with double-side dielectric DBRs was fabricated. Four discrete cavity modes were observed. The optical loss was 10^3 cm^{-1} order of magnitude and found to be mainly caused by the scattering of AlN/DBR interface. According to our calculation, the overlap coefficient between rough interface and stationary wave field, and roughness value of AlN interface were two critical parameters that contributed to the scattering loss in cavity. Our results may provide some helpful information for further refining the DUV VCSEL devices.

Acknowledgments

This work was supported by the National Key R&D Program of China (Grant No. 2016YFB0400803), the National Natural Science Foundation of China (Grant Nos. 11474235, U1505253, and 61704140), and the Science Challenge Project (Grant No. TZ2016003). Julien Brault, Samuel Matta, and Mathieu Leroux acknowledge partial support from the ANR Project <ANR-14-CE26-0025-01> "NANOGANUV."

References

1. M. Leroux et al., "Optical characterization of AlxGa1-xN alloys ($x < 0.7$) grown on sapphire or silicon," *Phys. Status Solidi B* **234**(3), 887–891 (2002).
2. K. Iida et al., "350.9 nm UV laser diode grown on low-dislocation-density AlGaN," *Jpn. J. Appl. Phys.* **43**(4A), L499–L500 (2004).
3. T. Takano et al., "Room-temperature deep-ultraviolet lasing at 241.5 nm of AlGaN multiple-quantum-well laser," *Appl. Phys. Lett.* **84**(18), 3567–3569 (2004).
4. M. Shatalov et al., "Room-temperature stimulated emission from AlN at 214 nm," *Jpn. J. Appl. Phys.* **45**(49), L1286–L1288 (2006).
5. M. Kneissl et al., "Ultraviolet semiconductor laser diodes on bulk AlN," *J. Appl. Phys.* **101**(12), 123103 (2007).
6. H. Yoshida et al., "Demonstration of an ultraviolet 336 nm AlGaN multiple-quantum-well laser diode," *Appl. Phys. Lett.* **93**(24), 241106 (2008).
7. V. N. Jmerik et al., "Low-threshold 303 nm lasing in AlGaN-based multiple-quantum well structures with an asymmetric waveguide grown by plasma-assisted molecular beam epitaxy on c-sapphire," *Appl. Phys. Lett.* **96**(14), 141112 (2010).
8. T. Wunderer et al., "Pseudomorphically grown ultraviolet C photopumped lasers on bulk AlN substrates," *Appl. Phys. Express* **4**(9), 092101 (2011).
9. V. N. Jmerik et al., "Plasma-assisted molecular beam epitaxy of AlGaN heterostructures for deep-ultraviolet optically pumped lasers," *Phys. Status Solidi* **210**(3), 439–450 (2013).
10. Z. Lochner et al., "Deep-ultraviolet lasing at 243 nm from photo-pumped AlGaN/AlN heterostructure on AlN substrate," *Appl. Phys. Lett.* **102**(10), 101110 (2013).
11. S. V. Ivanov et al., "Plasma-assisted molecular beam epitaxy of Al(Ga)N layers and quantum well structures for optically pumped mid-UV lasers on c-Al_2O_3," *Semicond. Sci. Technol.* **29**(29), 084008 (2014).

12. X.-H. Li et al., "Low-threshold stimulated emission at 249 nm and 256 nm from AlGaN-based multiple-quantum-well lasers grown on sapphire substrates," *Appl. Phys. Lett.* **105**(14), 141106 (2014).
13. M. Martens et al., "Performance characteristics of UV-C AlGaN-based lasers grown on sapphire and bulk AlN substrates," *IEEE Photonics Technol. Lett.* **26**(4), 342–345 (2014).
14. J. Yan et al., "Deep ultraviolet lasing from AlGaN multiple-quantum-well structures," *Phys. Status Solidi C* **13**(5-6), 228–231 (2016).
15. F. Koyama, "Advances and new functions of VCSEL photonics," *Opt. Rev.* **21**(6), 893–904 (2014).
16. K. Iga, "Vertical-cavity surface-emitting laser: Its conception and evolution," *Jpn. J. Appl. Phys.* **47**(1), 1–10 (2008).
17. K. Iga "VCSEL - its conception, development, and future," in *18th Micro-optics Conf. (Moc)*, p. 2, IEEE (2013).
18. K. Iga et al., "Surface emitting semiconductor-lasers," *IEEE J. Quantum Electron.* **24**(9), 1845–1855 (1988).
19. H. Soda et al., "GaInAsP/InP surface emitting injection lasers," *Jpn. J. Appl. Phys.* **18**(12), 2329–2330 (1979).
20. Y. Mei et al., "Tunable InGaN quantum dot microcavity light emitters with 129 nm tuning range from yellow-green to violet," *Appl. Phys. Lett.* **111**(12), 121107 (2017).
21. T. Hamaguchi et al., "Milliwatt-class GaN-based blue vertical-cavity surface-emitting lasers fabricated by epitaxial lateral overgrowth," *Phys. Status Solidi A* **213**(5), 1170–1176 (2016).
22. S. Izumi et al., "Room-temperature continuous-wave operation of GaN-based vertical-cavity surface-emitting lasers fabricated using epitaxial lateral overgrowth," *Appl. Phys. Express* **8**(6), 062702 (2015).
23. K. Omae et al., "Improvement in lasing characteristics of GaN-based vertical-cavity surface-emitting lasers fabricated using a GaN substrate," *Appl. Phys. Express* **2**, 052101 (2009).
24. T.-C. Lu et al., "CW lasing of current injection blue GaN-based vertical cavity surface emitting laser," *Appl. Phys. Lett.* **92**(14), 141102 (2008).
25. E. Feltin et al., "Blue lasing at room temperature in an optically pumped lattice-matched AlInN/GaN VCSEL structure," *Electron. Lett.* **43**(17), 924–926 (2007).
26. Y. Mei et al., "Quantum dot vertical-cavity surface-emitting lasers covering the 'green gap'," *Light: Sci. Appl.* **6**(1), e16199 (2016).
27. Y.-S. Liu et al., "Development for ultraviolet vertical cavity surface emitting lasers," *Proc. SPIE* **9748**, 974815 (2016).
28. H. Zhou et al., "Near ultraviolet optically pumped vertical cavity laser," *Electron. Lett.* **36**(21), 1777–1779 (2000).
29. J. M. Redwing et al., "An optically pumped GaN-AlGaN vertical cavity surface emitting laser," *Appl. Phys. Lett.* **69**(1), 1–3 (1996).
30. Y. S. Liu et al., "Optically pumped vertical-cavity surface-emitting laser at 374.9 nm with an electrically conducting n-type distributed Bragg reflector," *Appl. Phys. Express* **9**(11), 111002 (2016).
31. S. Matta et al., "Influence of the heterostructure design on the optical properties of GaN and $Al_{0.1}Ga_{0.9}N$ quantum dots for ultraviolet emission," *J. Appl. Phys.* **122**(8), 085706 (2017).
32. W. J. Liu et al., "Room temperature continuous wave lasing of electrically injected GaN-based vertical cavity surface emitting lasers," *Appl. Phys. Lett.* **104**(25), 251116 (2014).
33. D. Brunner et al., "Optical constants of epitaxial AlGaN films and their temperature dependence," *J. Appl. Phys.* **82**(10), 5090–5096 (1997).
34. K. H. Guenther et al., "Surface roughness measurements of low-scatter mirrors and roughness standards," *Appl. Opt.* **23**(21), 3820–3836 (1984).

Zhongming Zheng received his BS and ME degrees from Fuzhou University in 2014 and 2016, respectively. He is now a doctoral student at the Department of Electronic Engineering, Xiamen University. His research interests include III-nitride semiconductor material characterization and DUV optoelectronic devices.

Yingqian Li received her BE degree in 2015 from Northwest Polytechnical University. She is now a master student at the Department of Electronic Engineering, Xiamen University. Her research interests include III-nitride semiconductor material characterization and optoelectronic device fabrication.

Onkundi Paul received his bachelor and master degrees in 2009 and 2015 from Kenyatta University, Kenya. From 2016 to 2017, he was a physics assistant lecturer at Mwenge Catholic University, Tanzania. He joined the Department of Electronic Engineering, Xiamen University, in 2017, as a doctoral student. His research interests include DUV LEDs and their application in disinfection.

Hao Long received his BS and doctor degrees in 2008 and 2013 from Peking University, China. From 2013 to 2015, he was a staff researcher at Lenovo Inc., Beijing. From 2015 until now, he is an assistant professor at Xiamen University. He is dedicated in the research and development of III-nitride semiconductor material growth, device fabrication and characterization, and fundamental light–matter interaction in semiconductor microcavities.

Samuel Matta is a materials engineer graduated from Montpellier University with a masters degree in optoelectronics and microwaves. He also received a master's degree in applied physics from Claude Bernard University in Lyon. Currently, he is a PhD candidate in collaboration between Montpellier University and the National Center for Scientific Research (CNRS-CRHEA) working on the MBE growth of AlGaN based quantum dots for UV applications.

Mathieu Leroux is an engineer from the Ecole Supérieure de Physique et Chimie Industrielle de Paris. After his PhD on the MOVPE of antimonides, he entered the Centre National de la Recherche Scientifique as a researcher. He is mainly involved in the optical characterization of semiconductors or insulators, and the relations between materials optical properties and device characteristics. He is the author or coauthor of about 204 articles in physics journals.

Julien Brault is a specialist of semiconductor materials for optoelectronics. He presently works at the National Center for Scientific Research CNRS-CRHEA, on the MBE growth of nitride materials, in particular nanostructures (QDs, Q Wires, and QWs) on polar, non, and semipolar orientations, for visible and UV LEDs, photodetectors, and nonlinear optics. Earlier, he was involved with InP materials for telecom applications and Si QD MOSFET nonvolatile memories. He is the coauthor of 120 publications and 4 patents.

Leiying Ying received her BS degree from ZhongShan University, China and her ME degree in 1986 from Hebei Semiconductor Research Institute, China. She worked at RIKEN, Japan, for 6 years and joined Xiamen University in 2011. At present, she is a senior engineer in semiconductor devices. Her current research interests include micro-/nanofabrication and semiconductor devices for optoelectronic applications.

Zhiwei Zheng received his BE degree from Nanjing University of Science and Technology, Nanjing, China, in 2008, and his PhD degree from the Institute of Microelectronics of Chinese Academy of Sciences, Beijing, China, in 2014. He is currently an assistant professor with Xiamen University. His current research interests include nanofabrication and semiconductor devices for optoelectronic applications.

Baoping Zhang received his BS degree in 1983 from Lanzhou University, his ME degree in 1986 from HSRI, and his doctor degree in 1994 from University of Tokyo. His working experience includes 1986–1989: HSRI; 1994–1998: RIKEN, Japan; 1998-1999: Sharp Inc., Japan; and 1999–2006: RIKEN and JSTA, Japan. In 2006, he joined Xiamen University as a distinguished professor. He is engaged in wide gap semiconductors, especially GaN-based VCSELs.